# Effects of Microcrystalline Cellulose on Functional Properties of Hydroxy Propyl Methyl Cellulose Microcomposite Films

N. DOGAN AND T.H. MCHUGH

**ABSTRACT: Edible films and coatings in foods can be used to increase shelf-life and improve organoleptic characteristics of foods by avoiding deterioration of food components and therefore promoting preservation of the final product. This study is the first to investigate the use of different size fillers for the purpose of preparing edible composite films with fillers $< 1.0$ $\mu$m in size. For this purpose, water vapor permeability and mechanical properties of HPMC (hydroxy propyl methyl cellulose) based films with the inclusion of different size MCC (microcrystalline cellulose) fillers were studied. The water vapor permeability of the control HPMC film was $1.2 \pm 0.2$ g-mm/kPa-h-m$^2$ and did not show a significant change with the addition of fillers. A comparison of mechanical properties of the films with a tensile test showed that tensile strength of the control film, which was prepared using a 3 wt% HPMC solution, increased from $29.7 \pm 1.6$ MPa to $70.1 \pm 7.9$ MPa with the addition of 500-nm size particles, while it increased only to $37.4 \pm 5.5$ MPa with the addition of 3-$\mu$m size particles. Also important is that the elongation percentage of the control film did not decrease significantly with the addition of submicron size fillers to the HPMC films. This study showed that the increased surface area per weight of smaller size MCC fillers compared to their larger size counterparts was highly beneficial in terms of film mechanical property improvement.**

**Keywords: composite, films, HPMC, MCC, tensile strength, water vapor permeability**



## Introduction

The shelf-life and quality of most foods depend on the diffusion of moisture, fat, and aromas within the product or between the product and its exterior. Advantages of edible films and coatings in foods include improvement of shelf-life and organoleptic characteristics of foods by avoiding deterioration of food components and preservation of flavor and freshness, therefore promoting preservation of the food.

Edible films can prevent moisture migration and act as edible packaging materials or as layer coatings in heterogeneous processed foods. They can also improve the handling characteristics of the food by providing mechanical integrity (Perez-Gago and Krochta 2001). The main desired characteristics of an ideal edible film would be low water vapor permeability and high mechanical strength.

Many studies in food science have been involved in studying various edible films using proteins, polysaccharides, and lipids (Martin-Polo and others 1992; McHugh and Krochta 1994; Debeaufort and Voilley 1995; Handa and others 1999; Debeaufort and others 2000; Peres-Gago and Krochta 2001; Ghosh and others 2002; Phan and others 2002; Sothornvit and others 2002; Kim and others 2003; Hong and others 2004). These studies showed that hydrophobic substances such as lipids, varnishes, resins, essential oils, emulsifiers, and surface active agents are good moisture barriers but they form brittle films. Therefore, hydrophobic substances are generally combined with proteins or polysaccharides to form composite films in the form of bilayers or emulsion-based films in an effort to create barriers with desired mechanical strength and low permeability (Martin-Polo and others 1992; Debeaufort and Voilley 1995; Perez-Gago and Krochta 2001; Morillon and others 2002). The properties of bilayer and emulsion-based films have been reviewed by Debeaufort and others (1998), and Morillon and others (2002). The challenge today is still the relatively high permeability and poor mechanical integrity of edible composite films.

Composite materials with improved properties made from polymers reinforced with organic-based filler materials have received significant interest starting from the mid-1990s, when Favier and others (1995) showed that the addition of 3% to 6% crystalline cellulose in a copolymer acrylate latex film increased dynamic modulus by more than 3-fold. This effect of fillers on mechanical properties of polymers is consistent with the studies in which researchers have shown that the addition of nanosize organo-clay particles to polyamide based composites showed exceptional improvement in mechanical properties compared to their micron size counterparts (Yano and others 1993; Okada and Usuki 1995). During the last decade, these nano/micro composites with at least 1 component in the submicron size have found many applications in the automotive industry and packaging materials (Ke and others 1999).

Studies in nonfood usage of biopolymer-based films examined the effects of cellulose whiskers and cellulose micro/nano fibrils as functional fillers in these systems. (Angles and Dufresne 2000; Dufresne and others 2000). Inclusion of cellulose microfibrils in starch films reinforces the starch matrix regardless of the amount of plasticizer used. Despite these promising and attractive properties of packaging nanocomposites and cellulose fillers, the effect of nanosize microcrystalline cellulose (MCC) fillers in edible films is yet to be explored.

It is common in food science to form composite films with lipids using emulsification techniques but this study is the first to report the effect of cellulose fillers in sizes down to 500 nm in edible films. It

*MS 20060346 Submitted 6/16/2006, Accepted 10/14/2006.* *Authors are with Agricultural Research Service, Western Regional Research Center, 800 Buchanan St., Albany, CA 94710. Direct inquiries to author Dogan (E-mail: nihanda@gmail.com).*




doi: 10.1111/j.1750-3841.2006.00237.x

is an attempt to improve the mechanical properties of films without affecting their water vapor permeabilities by exploring the effect of MCC fillers in hydroxyl propyl methyl cellulose (HPMC) matrix. For this purpose, a film formed by drying 3 wt% HPMC solution was chosen as the control film and the main matrix for the other films with MCC fillers. Three different sizes of food-grade MCC filler materials at 2 different concentrations were blended into film forming HPMC solutions at 2 different shear rates. Water vapor permeability and mechanical properties of 12 composite films and the control film were analyzed.

## Materials and Methods

### Materials

HPMC film forming solution that forms the matrix gel in the films was prepared by dispersing HPMC in water using a high shear overhead stirrer for about an hour. HPMC (Methocel E15) was kindly provided by Dow (Dow Chemical Co., Midland, Mich., U.S.A.). Three different sizes of food grade 0.5, 1.5, and 3 $\mu$m MCC samples were kindly provided by FMC (FMC Biopolymers, Princeton, N.J., U.S.A.). The average sizes of MCC particles were measured using a light scattering particle size analyzer (Malvern Zetasizer, Malvern Instruments Inc., Southborough, Mass., U.S.A.).

### Film preparation

The control film was prepared using 3 wt% HPMC. The HPMC:water ratio in all film forming solutions was 3:97. In order to compare the effect of concentration of MCC in HPMC matrix, 2 different MCC/HPMC ratios were used in film compositions. The smallest size MCC sample was provided as an aqueous suspension and HPMC was mixed to the MCC suspension during the preparation of films. The 2 different ratios of MCC to HPMC in the dried films were 1:3 and 1:6. They were prepared by addition of 1.0 wt% and 0.5 wt% MCC in the film forming solutions. Also, 2 different films from each composition were prepared using an overhead stirrer and homogenizer at different mixing rates in order to compare the effect of shearing during the blending of fillers to the main matrix. Two different preparations were mixing with an overhead stirrer at 600 rpm for an hour and with a homogenizer at 10000 rpm for an hour. Table 1 presents the experimental design that consists of 12 tests.

After the solutions were prepared, vacuum was applied to degas film forming mixtures in order to prevent microbubble formation in the films. Glass casting plates (30 × 30 cm) with Mylar (Polyester film, Dupont, Hopewell, Va., U.S.A.) cover were used for film casting. The mixes were cast at a wet thickness of 0.5 mm onto plates using casting bars and the plates were placed on a leveled surface at room temperature and let dry for 24 h. After drying, the films were removed from the Mylar. Film thicknesses were measured with a digital micrometer (No. 7326, Mitutoyo Manufacturing, Japan) and 3 measurements along each film were recorded to calculate an average film thickness.

**Table 1 — Experimental design**

| Test | $X_1$ (Stirring speed) | $X_2$ (MCC:HPMC ratio) | $X_3$ (Particle size) |
|---|---|---|---|
| 1 | 600 rpm (−1) | 1:3 (+1) | 0.5 (−1) |
| 2 | 600 rpm (−1) | 1:3 (+1) | 1.5 (0) |
| 3 | 600 rpm (−1) | 1:3 (+1) | 3.0 (+1) |
| 4 | 600 rpm (−1) | 1:6 (−1) | 0.5 (−1) |
| 5 | 600 rpm (−1) | 1:6 (−1) | 1.5 (0) |
| 6 | 600 rpm (−1) | 1:6 (−1) | 3.0 (+1) |
| 7 | 10000 rpm (+1) | 1:3 (+1) | 0.5 (−1) |
| 8 | 10000 rpm (+1) | 1:3 (+1) | 1.5 (0) |
| 9 | 10000 rpm (+1) | 1:3 (+1) | 3.0 (+1) |
| 10 | 10000 rpm (+1) | 1:6 (−1) | 0.5 (−1) |
| 11 | 10000 rpm (+1) | 1:6 (−1) | 1.5 (0) |
| 12 | 10000 rpm (+1) | 1:6 (−1) | 3.0 (+1) |

### Microscopy

Scanning electron microscopy (SEM) observations were achieved with a Hitachi S-4700. SEM images were obtained using 2.0 kV. The specimens were mounted onto aluminum specimen stubs using double-stick carbon tabs (Ted Pella Inc., Redding, Calif., U.S.A.) and coated with gold/palladium on an ion sputter coater (Denton Vacuum Inc., Moorestwon, N.J., U.S.A.) for about 45 s at 20 mA, and images were taken.

### Mechanical property measurements

After drying, the films were conditioned at 33% RH for 72 h using a saturated solution at 23 °C ± 2 °C. This preconditioning before the tensile testing enables a true comparison of mechanical strength of the films. The films were then cut to have a rectangular midsection measuring 15-mm wide by 100-mm long, flaring to 25-mm by 35-mm square sections on each end.

An Instron Universal Testing Machine (Model 1122, Instron Corp., Canton, Mass., U.S.A.) was used to determine the maximum TS (tensile strength), maximum percentage elongation at break (%), and elastic modulus (also called Young's modulus). The instrument was operated with self-alignment grips that consist of 1 fixed and 1 free end. The free end moves easily into alignment when load is applied. The mechanical properties were determined at room temperature according to ASTM D882-97. The ends of the cut films were clamped with grips and films were stretched using a speed of 50 mm/min. Testing conditions were 33% ± 2% RH and 23 °C ± 2 °C. The strain is determined by

$$\varepsilon = \ln(L/L_0) \quad (1)$$

where L and $L_0$ are the length during the test and the initial length, respectively. The stress is calculated by

$$\sigma = F/S \quad (2)$$

where F is the applied load and S is the cross-sectional area of the film.

Elongation at break is the percentage change in the original film length between the grips. The final length is measured when the film breaks. Elastic modulus is calculated from the slope of the initial linear region of stress–strain curve. Tensile strength is the maximum stress a film can withstand against applied tensile stress before the film tears. It is calculated by dividing the maximum load at break by cross-sectional area of the film. The mechanical properties of the films were analyzed as a function of particle size, method of mixing and concentration.

### Water vapor permeability measurements

Water vapor permeability was determined using ASTM E96-00 and corrections for air gap inside the cups were included in the calculations. This correction is necessary as the ASTM E96-00 is based on the assumption that relativity humidity is 100% under the film in the test cup. Three films were cast for each film formulation and average water vapor permeability was calculated to prevent the effect of defects on the water vapor permeability testing. Circular test cups and controlled air desiccating/climate-controlled cabinets were used in water vapor permeability measurements. The test cups were made of polymethylmethacrylate (Plexiglass) in the Food Science and Technology Dept. at Univ. of California, Davis. A fan was built into desiccating cabinets in order to provide proper air circulation. Temperature was kept as 25 °C and relative humidity was kept

at 50% in the cabinets. The films were cut in spherical shape (5-cm dia) and were mounted in the test cups, which were filled with 6 mL deionized water. The cups were then sealed with silicon sealant and 4 screws were placed around the cup circumference. In this configuration, the only area through which water can permeate is the film surface. The cups were placed in climate-controlled cabinets, the weight of cups was measured over time, and water vapor permeability through the films was calculated. The weight measurements were recorded at 2-h intervals for a 36-h period.

Water vapor flux was calculated by dividing water vapor transmission rate, which is slope of weight loss compared with time curve, by the area through which water can permeate. Water vapor permeability was calculated using the mean final film thickness, water vapor flux, vapor pressure of water at 25 °C, and a correction for the relative humidity difference between the cup interior and the cabinet. A modification of the ASTM E-96-95 was employed and the relative humidity at the cup interior was calculated using Eq. 3 to 5:

$$\text{Water vapor transmission rate(WVTR)} = \text{weight loss per time/film area} \quad (3)$$

$$\text{WVTR} = \frac{mw\text{PDln}[(P - p_2)/(P - p_1)]}{\text{RT}z} \quad (4)$$

$$\text{RH}_{\text{underside}} = \frac{p_2}{p_1} \times 100 \quad (5)$$

where $mw$ is the molecular weight of water (18 g/gmol), $P$ is total pressure (1 atm), $D$ is diffusivity of water vapor through air at 298 K (0.102 $m^2$/s), $p_1$ is saturation pressure vapor at 298 K (0.0313 $m^2$/s), $p_2$ is water vapor partial pressure at underside of the film, R is gas constant (82.1 $\times 10^{-6}$ $m^3$atm/gmolk), and $z$ is the height of mean stagnant air gap.

Water vapor permeability (WVP) was calculated using the following relation:

$$\text{WVP} = \frac{\text{WVTR}}{(p_2 - p_3)}y \quad (6)$$

where $y$ is average film thickness and $p_3$ is water vapor partial pressure at the upper side of the film.

### Statistical analysis of data

Water vapor permeability is measured as the mean of 3 repetitions and standard deviations were reported. Mechanical properties of films were reported as the means of 5 film repetitions. Analysis of variance (ANOVA) and multiple comparison tests were applied using Minitab 14.2 (Minitab Inc., State College, Pa., U.S.A.) to study the interactions and effects of particle size, concentration, and preparation on film properties.

## Results and Discussions

### Size analysis and scanning electron microscopy

The mean particle sizes of MCC samples were measured as 0.5, 1.5, and 3 $\mu$m using a light scattering particle size analyzer (Malvern Zetasizer). Scanning electron microscopy (SEM) was used to characterize the morphology of the composite films. Figure 1a represents a SEM micrograph of our control film, which was unloaded and prepared with a solution of 3 wt% HPMC in water. The shape of filler particles is rod-like as shown in Figure 1b, which represents a SEM micrograph of a film with 0.5-$\mu$m average size MCC in HPMC matrix. The ratio of MCC to HPMC in this particular film was 1 part MCC to 6 parts of HPMC. The distance between each bar in the scales in Figure 1a and 1b is 2 $\mu$m. As the diameters of these particles were in submicron range, they are referred as nanofibers. These particles in water hold their structure with strong intramolecular and intrastrand hydrogen bonds that form crystals that are insoluble in aqueous solutions.

In some regions of SEM micrographs of MCC nanofibers, fibers in the films prepared using a high shear homogenizer seem to be more aligned in comparison to those prepared using a low shear overhead stirrer. This can be observed in Figure 1b. However, it was not enough to conclude a significant difference between the SEM images of films having the same composition but different mixing methods.

### Effect of fillers on water vapor permeability of composite films

Effect of preparation method as well as size and concentration of MCC on water vapor permeability of films was studied. The water vapor permeability of the control HPMC film was 1.2 ± 0.2 g-mm/kPa-h-$m^2$. Table 2 shows a comparison of permeability results. As it can be seen in Table 2, there was not any significant change in water vapor permeability of the films with the preparation method, size, and concentration of MCC in the films. The water vapor permeability of all films was found to be about 1.25 ± 0.1 g-mm/kPa-h-$m^2$. Dufresne and others (2000) previously reported a decreased diffusion coefficient for starch films embedded with cellulose microfibrils. A decrease in diffusion coefficient is expected with the addition of cellulose fibrils as the diffusion of water in the films depends on the available pathways for water molecules. However, it is possible that a decrease in diffusion coefficient alone is not enough to see a noticeable difference in water vapor permeability of these composite films. The structure of films with fillers could be providing a more

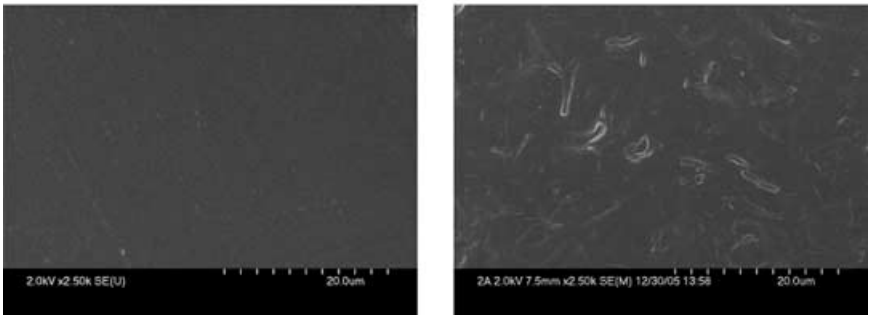


**Figure 1—(a) Scanning electron micrograph of the control film (prepared with 3 wt% aqueous HPMC solution). (b) Scanning electron micrograph of a film with 0.5 $\mu$m average size MCC in HPMC matrix. MCC to HPMC ratio in this film was 1 of 6 (prepared with 3 wt% aqueous HPMC solution). The filler-matrix suspension that was used to prepare this film was prepared by blending the fillers with the matrix using high shear mixing at 10000 rpm.**

**Table 2—Comparison of water vapor permeability (WVP) of films**

| Film type | Thickness (mm) | RH (%) | WVT rate (g/h-m$^2$) | Permeability (g-mm/kPa-h- m$^2$) |
|---|---|---|---|---|
| Control (3 wt% HPMC) | 0.03 ± 0.002 | 65 ± 3 | 80.7 ± 7.1 | 1.2 ± 0.2 |
| MCC:HPMC (600 rpm) | | | | |
| 1.0:6.0 (3 $\mu$m MCC) | 0.04 ± 0.007 | 67 ± 3 | 77.5 ± 7.2 | 1.3 ± 0.1 |
| 1.0:3.0 (3 $\mu$m MCC) | 0.04 ± 0.005 | 71 ± 2 | 68.4 ± 5.9 | 1.4 ± 0.1 |
| 1.0:6.0 (1.5 $\mu$m MCC) | 0.04 ± 0.003 | 70 ± 1 | 70.8 ± 3.4 | 1.3 ± 0.2 |
| 1.0:3.0 (1.5 $\mu$m MCC) | 0.04 ± 0.008 | 73 ± 4 | 63 ± 10 | 1.1 ± 0.1 |
| 1.0:6.0 (0.5 $\mu$m MCC) | 0.03 ± 0.003 | 67 ± 1 | 76.2 ± 5.6 | 1.2 ± 0.1 |
| 1.0:3.0 (0.5 $\mu$m MCC) | 0.04 ± 0.005 | 67 ± 4 | 76 ± 6 | 1.3 ± 0.1 |
| MCC:HPMC (10000 rpm) | | | | |
| 1.0:6.0 (3 $\mu$m MCC) | 0.03 ± 0.002 | 72 ± 3 | 71.9 ± 12.3 | 1.0 ± 0.2 |
| 1.0:3.0 (3 $\mu$m MCC) | 0.04 ± 0.005 | 69 ± 3 | 65.2 ± 6.5 | 1.4 ± 0.1 |
| 1.0:6.0 (1.5 $\mu$m MCC) | 0.03 ± 0.002 | 70 ± 5 | 70.1 ± 6 | 1.1 ± 0.2 |
| 1.0:3.0 (1.5 $\mu$m MCC) | 0.05 ± 0.01 | 74 ± 2 | 61.4 ± 3.5 | 1.2 ± 0.3 |
| 1.0:6.0 (0.5 $\mu$m MCC) | 0.04 ± 0.01 | 70 ± 3 | 70 ± 7.1 | 1.4 ± 0.2 |
| 1.0:3.0 (0.5 $\mu$m MCC) | 0.05 ± 0.006 | 72 ± 2 | 64 ± 5.4 | 1.4 ± 0.1 |

compact structure with decreased diffusivity but could also be more favorable to water molecules with higher water affinity. The driving force for water migration is water concentration gradient and the factors describing the permeability process include interaction between the migrant and the food system (sorption/desorption) and microstructure of the food matrix.

## Effect of preparation method on mechanical properties

Table 3 shows the results of elongation and tensile strength from all the tests. This table clearly demonstrates the reinforcing effect of MCC fillers. Increase in tensile strength of films varied from 10% with the addition of 1.5- and 3.0-$\mu$m MCC fibers to over 100% with the addition of MCC nanofibers to HPMC films. The tensile strength of the control film increased from 28.5 ± 1.5 to 70.1 ± 7.9 MPa with the addition of 0.5-$\mu$m MCC nanofibers to the HPMC film forming solution using a homogenizer.

Table 4 shows results from the analysis of the effects of particle size (PS), stirring speed (SS), and concentration (C) on the mechanical properties of films. Significant effects of stirring speed were observed for the elastic modulus and tensile strength of the films. The tensile strength of films was higher when MCC fillers were blended with HPMC matrix using a homogenizer at 10000 rpm instead of an overhead stirrer at 600 rpm.

Figure 2 and 3 demonstrate the change in elongation and tensile strength, respectively, as a function of stirring speed and particle size.

**Table 3—Comparison of elongation and tensile strength of films**

| Film type | Elongation (%) | Tensile strength (MPa) |
|---|---|---|
| Control (3 wt% HPMC) | 9.6 ± 1.1 | 28.5 ± 1.5 |
| MCC:HPMC (600 rpm) | | |
| 1.0:6.0 (3 $\mu$m MCC) | 7.7 ± 1.7 | 30.1 ± 1.7 |
| 1.0:3.0 (3 $\mu$m MCC) | 4.0 ± 0.4 | 37.3 ± 5.8 |
| 1.0:6.0 (1.5 $\mu$m MCC) | 7.9 ± 2.4 | 34.2 ± 5.8 |
| 1.0:3.0 (1.5 $\mu$m MCC) | 4.6 ± 1.3 | 28.9 ± 2.2 |
| 1.0:6.0 (0.5 $\mu$m MCC) | 8.5 ± 2.2 | 56.5 ± 5.1 |
| 1.0:3.0 (0.5 $\mu$m MCC) | 5.4 ± 1.3 | 54.5 ± 5.2 |
| MCC:HPMC (10000 rpm) | | |
| 1.0:6.0 (3 $\mu$m MCC) | 4.7 ± 1.9 | 37.3 ± 5.5 |
| 1.0:3.0 (3 $\mu$m MCC) | 4.8 ± 0.7 | 37.2 ± 2.2 |
| 1.0:6.0 (1.5 $\mu$m MCC) | 4.8 ± 0.6 | 48.6 ± 5.5 |
| 1.0:3.0 (1.5 $\mu$m MCC) | 6.6 ± 2.2 | 55 ± 2.6 |
| 1.0:6.0 (0.5 $\mu$m MCC) | 11.5 ± 5.2 | 52.9 ± 4.2 |
| 1.0:3.0 (0.5 $\mu$m MCC) | 8.9 ± 2.1 | 70.1 ± 7.9 |

Although stirring speed alone did not have a significant effect on elongation, interaction effects of stirring speed and particle size were observed for elongation. As can be observed in Figure 2, the elongation did not change significantly with the stirring speed for films with 1.5 and 3.0-$\mu$m fibers, whereas a high stirring speed and low particle size, in nanosize, resulted in an elongation percentage at break that is close to the elongation percentage of the control film. This interaction of particle size and stirring can be clearly seen in Figure 2. The increased interaction area of well-aligned and homogeneously dispersed MCC nanofibers could be exerting a plasticizing effect of sorts whereby the elongation is maintained at the level of the control samples. In general, smaller molecular size of plasticizers increases the effectiveness of the plasticizers (Zhang and Han 2006).

Figure 3 shows that tensile strength increased with increased stirring speed. These results show that the amount of applied shear during the preparation of composite film forming solution can have a significant effect on mechanical properties of composite films. For example, the tensile strength of films with 1.0 part 1.5 $\mu$m MCC in 6 parts HPMC prepared by the overhead stirrer was 34.2 ± 5.8 MPa, whereas the same composition film that was mixed using a homogenizer was 48.6 ± 5.5 MPa. Using high shear with a homogenizer, MCC particles are probably better separated and rather individually dispersed in the matrix suspension. This could enable homogeneous distribution of tensile strength on the rod-shaped MCC particles as well as increased surface area for hydrogen bonding. The highest tensile strength was observed with the film that was prepared using a homogenizer and nanosize MCC. The tensile strength of films with 1 part 0.5 $\mu$m MCC to 3 parts HPMC prepared by the overhead stirrer was 54.5 ± 5.2 MPa, whereas the same composition film that was mixed using a homogenizer was 70.1 ± 7.9 MPa. The tensile strength of the control film was 28.5 ± 1.5 MPa.

**Table 4—ANOVA results for elongation (E), elastic modulus (EM), and tensile strength (TS)**

| | *F* value | | |
|---|---|---|---|
| Variable | E | EM | TS |
| Stirring speed (SS) | 1.05 | 84.15* | 72.33* |
| Particle size (PS) | 8.96* | 36.11* | 118.88* |
| MCC concentration (C) | 8.03* | 0.25 | 4.47* |
| Interaction SS-PS | 4.88* | 14.29* | 7.97* |
| Interaction PS-C | 0.7 | 5.08 | 14.53* |
| Interaction SS-C | 5.06* | 0.02 | 4.92* |
| Interaction SS-C-PS | 1.26 | 8.94* | 5.05* |

*Significant at $P \leq 0.05$.

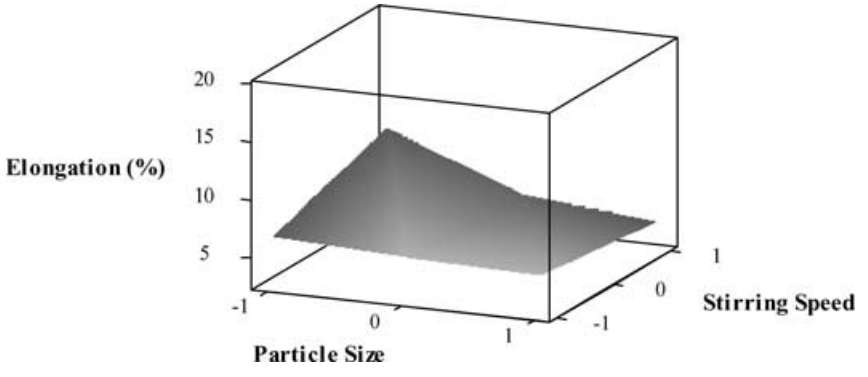


**Figure 2—Change in elongation as a function of particle size and stirring speed**

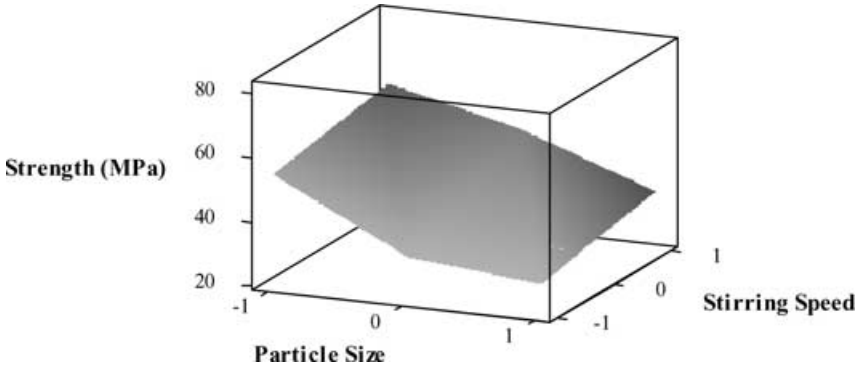


**Figure 3—Change in tensile strength as a function of particle size and stirring speed**

Figure 4 shows the effect of stirring speed on elastic modulus. As concentration alone did not have a significant effect on elastic modulus (Table 4), Figure 4 only represents the data at 1 concentration. The elastic modulus of the controlled film was 1001 ± 46.6 MPa. Pair-wise comparison of films showed a significant difference in the elastic modulus of films prepared by mixing at 2 different shear rates. Overall, homogenized samples showed increased strength and brittleness. An interesting observation was the interaction of stirring speed and particle size on elongation and elastic modulus. Although the film with 0.5 $\mu$m MCC had an elastic modulus almost double the elastic modulus of the control film, the film that was prepared with homogenization did not show a significant change in elongation in comparison with the control film.

## Effect of size and concentration on mechanical properties

Figure 5 shows a comparison of tensile strength of films with particle size and concentration. The tensile strength increased with the addition of fillers in all films. The effect of concentration was significant when particles less than 1.0 $\mu$m were used as fillers. Particle size effect was significant as was the interaction effect of particle size and concentration (Table 4). Tensile strength of films increased dramatically with concentration when 500 nm MCC was used. It is not unexpected that the effect of concentration of fillers would be more pronounced at high concentrations of small size fillers as the biggest difference of small size fibers to bigger size fibers is their remarkably high surface area per weight.

The effectiveness of the reinforcing effect of MCC in HPMC films is evident in Figure 5. The effect of particle size on mechanical properties has been shown to be remarkable. This result is in agreement with results from polymer nanocomposites. Polymer composites with well-dispersed nanometer size $TiO_2$ particles at 10% loading have increased resistance to scratching, whereas micron filled composites did not show any increase in scratch resistance and strain-to-failure decreased (Ng and others 2001).

As the particle size decreased, the increase in tensile strength increased dramatically. The highest tensile strength of films was achieved in films with 1 part 0.5 $\mu$m MCC fillers to 3 parts HPMC (highest concentration and smallest MCC size). It is important to note that the tensile strength of this film was in the same range as PET films. The tensile strength of HPMC control film was 28.5 ± 1.5 MPa. This is in very good agreement with the previously reported

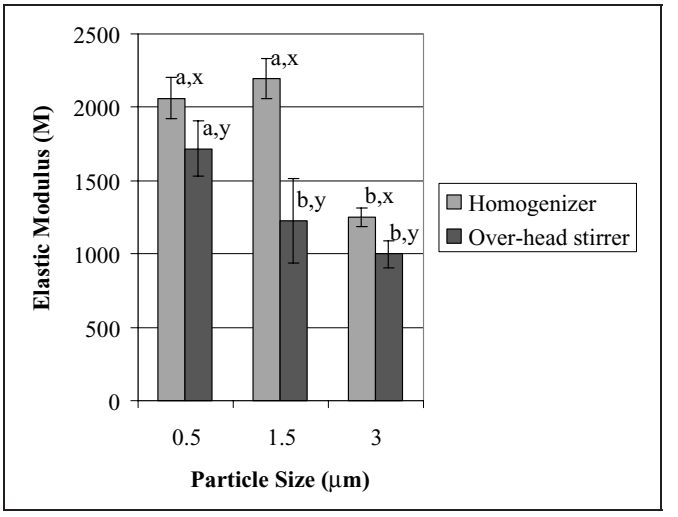


**Figure 4—Effect of particle size and preparation method on elastic modulus of MCC/HPMC: 1 of 6 composite films. Values are means and error bars indicate the standard deviations. First letters represent statistical comparison made independently for 2 preparation methods and means with the same letters are not significantly different ($P < 0.05$). Second letters represent statistical comparison made independently at each particle size and means with the same letters are not significantly different ($P < 0.05$).**

results for HPMC films. Sebti and others (2003) reported the tensile strength of films prepared from 3 wt% HPMC solution to be 32 ± 6 MPa.

The tensile strength of the control HPMC film increased from 28.5 ± 1.5 MPa to 70.1 ± 7.9 MPa with the addition of 1 part 0.5 $\mu$m MCC fillers to 3 parts HPMC, while tensile strength increased only to 37.3 ± 5.8 MPa with the addition of 1 part 3.0-$\mu$m MCC fillers to 3 parts HPMC. This effect may be explained by 2 reasons. First, it can be proposed that the increased surface area of smaller size MCC fillers compared to their larger size counterparts increases the hydrogen bonding of MCC with the matrix gel. As the water evaporates during film formation, the MCC filler-HPMC composite network forms by the establishment of hydrogen bonding. Hence, the increased surface area reinforces the structure. It is possible that this increased hydrogen bonding enables increased share and distribution of tensile force on individual rod-like MCC particles during tensile testing. This result shows that the larger the surface area per weight, the stronger the bonding between the fillers and the matrix, thereby the increased involvement of individual MCC rod-like particles in handling the applied load. Second, the bigger size particles may be disturbing the gel formation of HPMC during drying while they still help to increase tensile strength with new bonds. This would also explain why the tensile strength of films with the biggest particle size did not increase with an increase in concentration. The average percentage increase in tensile strength of films with an increase in the weight ratio of MCC/HPMC was 13% and 32% for 1.5 $\mu$m MCC and 0.5 $\mu$m MCC particle embedded films, respectively. There was no significant difference in tensile strength of the films at different concentrations of 3 $\mu$m MCC. At this high concentration, it is possible that the positive effect of increased number of MCC particles were suppressed by the negative effect they had on HPMC gel formation. Compatibility of the filler materials with the main gel matrix that is forming the film such as the steric effects and homogeneous distribution of filler materials are critical factors effecting composite film properties (Maiti and others 2002). Size, configuration, and compatibility of MCC filler materials with the main HPMC matrix define the functional properties of the films.

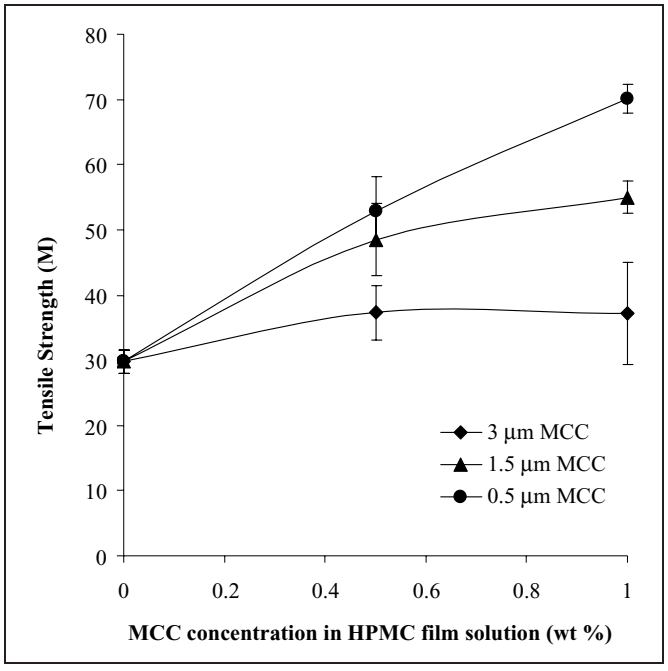


**Figure 5—Tensile strength of films at different size and concentration of MCC. Values show the means and error bars indicate the standard deviations.**

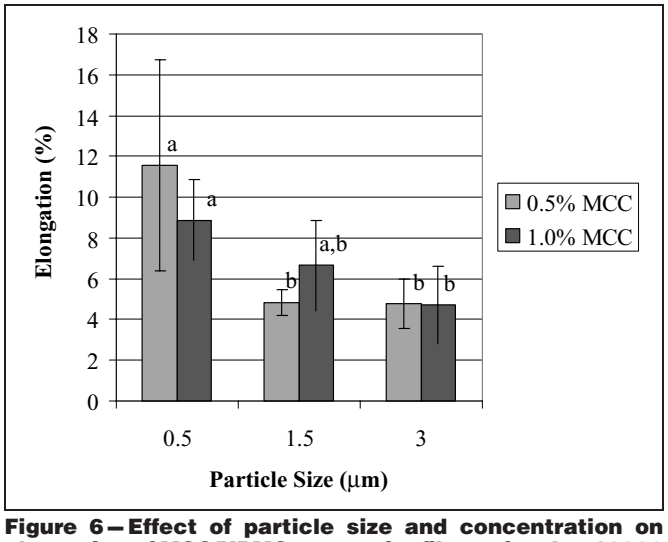


**Figure 6—Effect of particle size and concentration on elongation of MCC/HPMC composite films stirred at 10000 rpm. Values are means and error bars indicate the standard deviations. Letters represent statistical comparison made independently for 2 concentrations and means with the same letters are not significantly different ($P < 0.05$).**

Figure 4 shows the effect of particle size on elastic modulus. The concentration did not have a significant effect on elastic modulus (Table 4). The elastic modulus of the control was 1001 ± 47 MPa. The highest elastic modulus measured with the addition of 1 part 0.5-$\mu$m MCC fillers to 3 parts HPMC was 2175 ± 424 MPa. It is normally expected that as the elastic modulus increases, the percentage of elongation at break decreases as the films become stiffer. Figure 6 shows the elongation at break as a function of particle size and concentration for the films prepared with a homogenizer. The percentage elongation of the control HPMC film was 9.6% ± 1.1%. As can be seen in Figure 2, elongation percentage of all the films decreased when the film mixes were prepared at low shear. There was no significant difference in the elongation percentage of MCC embedded films when MCC was mixed to HPMC solution at low shear. The percentage elongation of films decreased to about 30%. However, as discussed in the previous section, the interaction effects of particle size and preparation method were obvious (Figure 2). One of the very important results in this study was observed with the changes in percentage elongation at break of films that were prepared with a homogenizer. Elongation percentage of the 0.5 $\mu$m MCC embedded films did not change dramatically. The percentage elongation of films with 1 part 0.5 $\mu$m to 3 parts HPMC film was found to be 11.6% ± 5.2%. It was 8.9% ± 1.9% when the MCC to HPMC ratio was 1 to 6 parts. This is very promising as the addition of submicron size fillers has the desirable effect of improving the overall tenacity of the films.

## Conclusions

This study is the first to investigate the use of nanosize MCC fillers for the purpose of preparing edible microcomposite films. It was shown that through the incorporation of fillers such as MCC, edible film mechanical properties can be significantly improved without reducing film barrier properties. These findings are expected to have a significant impact on the food industry by enabling them to manufacture edible films with improved tensile strengths, while maintaining their elongation and water vapor permeability values. The size, configuration, and water bonding properties of filler materials as well as their compatibility with the matrix affect the microstructure and overall functional properties of films. These results will allow

food scientists to envision a new generation of composite edible films and barriers and not be restricted to emulsified and bilayer films for current and new applications.

## Acknowledgments

The authors would like to acknowledge and thank Dr. Greg Krawczyk and his research group at FMC Biopolymers R&D for providing the materials and fruitful discussions. Also, authors would like to acknowledge Dr. Roberto A. Bustillos for his assistance with statistical analysis and BCE, ARS, for the SEM images.

## References

Angles MN, Dufresne A. 2000. Plasticized starch/tunicin whisker nanocomposites. 1. Structural analysis. Macromolecules 33:8344–53.

Debeaufort F, Voilley A. 1995. Effect of surfactants and drying rate on barrier properties of emulsified edible films. Int J Food Sci 30:183–90.

Debeaufort F, QuezadaGallo JA, Voilley A. 1998. Edible films and coatings: tomorrow's packagings: a review. Crit Rev Food Sci Nutr 38:299–313.

Debeaufort F, QuezadaGallo JA, Delporte B, Voilley A. 2000. Lipid hydrophobicity and physical state effects on the properties of bilayer edible films. J Memb Sci 180:47–55.

Dufresne A, Dupeyre D, Vignon MR. 2000. Cellulose microfibrils from potato tuber cells: processing and characterization of starch-cellulose microfibril composites. J Appl Poly Sci 76:2080–92.

Favier V, Cavaille JY, Canova GR, Shrivastava SC. 1995. Mechanical percolation in cellulose whisker nanocomposites. Polym Eng Science 37 (10):1732–9.

Ghosh V, Ziegler GR, Anantheswaran RC. 2002. Fat, moisture, and ethanol migration through chocolates and confectionary coatings. Crit Rev Food Sci Nutr 42(6):583–626.

Handa A, Gennadios A, Hanna MA, Weller CL, Kuroda N. 1999. Physical and molecular properties of egg-white lipid films. J Food Sci 64(5):860–4.

Hong SI, Han JH, Krochta JM. 2004. Optical and surface properties of whey protein isolate coatings on plastic films as influenced by substrate, protein concentration, and plasticizer type. J Appl Polym Sci 92(1):335–43.

Ke Y, Long C, Qi Z. 1999. Crystallization, properties, and crystal and nanoscale morphology of PET-clay nanocomposites. J Appl Polym Sci 71:1139–46.

Kim KM, Marx DB, Weller CL, Hann MA. 2003. Influence of sorghum wax, glycerin, and sorbitol on physical properties of soy protein isolate films. J Am Oil Chem Soc 80(1):71–6.

Maiti P, Yamada K, Okamoto M, Ueda K, Okamoto K. 2002. New polylactide/layered silicate nanocomposites: role of organoclays. Chem Mater 14:4654–61.

Martin-Polo M, Mauguin C, Volley A. 1992. Hydrophobic films and their efficiency against moisture transfer.1. Influence of the film preparation technique. J Agric Food Chem 40:407–12.

McHugh TH, Krochta JM. 1994. Dispersed phase particles-size effects on water-vapor permeability of whey-protein beeswax edible emulsion films. J Food Process Preserv 18:173–88.

Morillon V, Debeaufort F, Blond G, Capelle M, Voilley A. 2002. Factors affecting the moisture permeability of lipid-based edible films: a review. Crit Rev Food Sci Nutr 42 (1):67–89.

Ng CB., Ash BJ, Schadler LS, Siegel RW. 2001. A study of the mechanical and permeability properties of nano- and micron-$TiO_2$ filled epoxy composites. Adv Composites Lett 10(3):101–11.

Okada A, Usuki A. 1995. The chemistry of polymer-clay hybrids. Matter Sci Eng C 3:109–15.

Peres-Gago MB, Krochta JM. 2001. Lipid particle size effect on water vapor permeability and mechanical properties of whey protein/beeswax emulsion films. J Agric Food Chem 49:996–1002.

Phan DT, Debeaufort F, Peroval C, Despre D, Courthaudon JL, Voilley A. 2002. Arabinoxylan-lipid-based edible films and coatings. 3. Influence of drying temperature on film structure and functional properties. J Agric Food Chem 50:2423–8.

Sebti I, Delves-Broughton J, Coma V. 2003. Physicochemical properties of bioactivity of nisin-containing cross-linked hydroxypropylmethylcellulose films. J Agric Food Chem 51:6468–74.

Sothornvit R, Reid DS, Krochta JM. 2002. Plasticizer effect on the glass transition temperature of beta-lactoglobulin films. Trans ASAE 45:1479–84.

Yano K, Usuki A, Okada A, Kurauchi T, Kamigaito O. 1993. Synthesis and properties of polyimide clay hybrid. J Polym Sci: Part A: Polym Chem 31:2493–8.

Zhang Y, Han JH. 2006. Mechanical and thermal characteristics of pea starch films plasticized with monosaccharides and polyols. J Food Sci 71(2):109–18.